Regular Article

❤ blood

THROMBOSIS AND HEMOSTASIS

Gut microbiota regulate hepatic von Willebrand factor synthesis and arterial thrombus formation via Toll-like receptor-2

Sven Jäckel,[1,2] Klytaimnistra Kiouptsi,[1] Maren Lillich,[1] Tim Hendrikx,[3,4] Avinash Khandagale,[1] Bettina Kollar,[1] Nives Hörmann,[1] Cora Reiss,[1] Saravanan Subramaniam,[1] Eivor Wilms,[1] Katharina Ebner,[5] Marie-Luise von Brühl,[6] Philipp Rausch,[7] John F. Baines,[7,8] Sandra Haberichter,[9-11] Bernhard Lämmle,[1,12] Christoph J. Binder,[3,4] Kerstin Jurk,[1,2] Zaverio M. Ruggeri,[13] Steffen Massberg,[6] Ulrich Walter,[1,2] Wolfram Ruf,[1,2,14] and Christoph Reinhardt[1,2]

[1]Center for Thrombosis and Hemostasis, University Medical Center, Johannes Gutenberg University of Mainz, Mainz, Germany; [2]German Center for Cardiovascular Research, Partner Site Rhein-Main, Mainz, Germany; [3]CeMM Research Center for Molecular Medicine of the Austrian Academy of Sciences, Vienna, Austria; [4]Department of Laboratory Medicine, Medical University of Vienna, Vienna, Austria; [5]III. Medical Clinic and Polyclinic, University Medical Center, Johannes Gutenberg University of Mainz, Mainz, Germany; [6]Medical Clinic and Polyclinic I, Clinic of the Ludwig-Maximilians-University Munich, Munich, Germany; [7]Max Planck Institute for Evolutionary Biology, Plön, Germany; [8]Institute for Experimental Medicine, University of Kiel, Kiel, Germany; [9]Diagnostic Laboratories and [10]Blood Research Institute, BloodCenter of Wisconsin, Milwaukee, WI; [11]Department of Pediatrics, Medical College of Wisconsin, Milwaukee, WI; [12]Clinic of Hematology and Central Hematology Laboratory, Inselspital University Hospital, Bern, Switzerland; and [13]Department of Molecular Medicine and [14]Department of Immunology and Microbiology, The Scripps Research Institute, La Jolla, CA

Key Points

- VWF synthesis in liver endothelial cells is regulated by gut microbiota through TLR2 signaling.

- Reduced plasma VWF levels in GF and *Tlr2*⁻/⁻ mice cause reduced thrombus formation at the ligation-injured carotid artery.

The symbiotic gut microbiota play pivotal roles in host physiology and the development of cardiovascular diseases, but the microbiota-triggered pattern recognition signaling mechanisms that impact thrombosis are poorly defined. In this article, we show that germ-free (GF) and Toll-like receptor-2 (*Tlr2*)-deficient mice have reduced thrombus growth after carotid artery injury relative to conventionally raised controls. GF *Tlr2*⁻/⁻ and wild-type (WT) mice were indistinguishable, but colonization with microbiota restored a significant difference in thrombus growth between the genotypes. We identify reduced plasma levels of von Willebrand factor (VWF) and reduced VWF synthesis, specifically in hepatic endothelial cells, as a critical factor that is regulated by gut microbiota and determines thrombus growth in *Tlr2*⁻/⁻ mice. Static platelet aggregate formation on extracellular matrix was similarly reduced in GF WT, *Tlr2*⁻/⁻, and heterozygous *Vwf*⁺/⁻ mice that are all characterized by a modest reduction in plasma VWF levels. Defective platelet matrix interaction can be restored by exposure to WT plasma or to purified VWF depending on the VWF integrin binding site. Moreover, administration of VWF rescues defective thrombus growth in *Tlr2*⁻/⁻ mice in vivo. These experiments delineate an unexpected pathway in which microbiota-triggered TLR2 signaling alters the synthesis of proadhesive VWF by the liver endothelium and favors platelet integrin–dependent thrombus growth. (*Blood*. 2017;130(4):542-553)

Introduction

The commensal microbiota are an environmental factor that alters host physiology. Even with intact gut barrier function, pathogen-associated molecular patterns derived from gut microbial communities, such as peptidoglycan (PG)[1] and lipopolysaccharides[2] constantly leak into tissues and the portal circulation,[3] triggering adaptive Toll-like receptor (TLR) signaling in the host. Host-microbial symbiosis changes cellular immune function in the gut, but also systemically.[4,5] However, TLR signaling is not restricted to the innate immune system,[6] but also involves cellular pathways relevant to hemostasis and thrombosis in endothelial cells (TLR2, 4, and 9)[7-9] and platelets (TLR1, 2, 4, 6, and 9).[10-13] In addition, the fecal metagenome of symptomatic atherosclerosis patients is characterized by enrichment of genes encoding PG biosynthesis, thus triggering TLRs.[14]

Innate immune defense mechanisms prevent dissemination of microbes and localize bacterial infection through the extrinsic tissue factor coagulation pathway.[15] Platelets also act as a central evolutionary link between innate immune responses and hemostatic functions and respond to TLR ligands.[16] TLR2 and TLR4 are linked to platelet activation and contribute to innate defense mechanisms by promoting the generation of prothrombotic extracellular nucleosomes and histones associated with neutrophil extracellular traps.[17] TLR2 stimulation directly evokes platelet responses,[17-21] mediates endothelial responses to pathogen-associated molecular patterns, and can promote coagulation by endothelial cells.[22] However, it is not fully understood how TLRs contribute to thrombosis in vivo[13,18,21] and whether TLR sensing by the endothelium regulates thrombogenesis under steady-state or challenge conditions.[22]

Endothelial cell von Willebrand factor (VWF) release and P-selectin externalization are triggered by TLR2/6.[23] The multimeric protein VWF plays a key role in hemostasis and thrombosis.[24,25] VWF is

---

released into blood and the subendothelium[26] by endothelial cells[27] and packaged into platelet α-granules[28] by megakaryocytes.[29] At sites of vascular injury, plasma VWF promotes platelet adhesion to the extracellular matrix and platelet aggregation,[30] in particular as wall shear rates increase.[31] Subendothelial VWF supports platelet adhesion,[32] whereas platelet-released VWF is not essential for hemostasis.[33,34] VWF multimers vary in size from 5×10^5 to $>5 \times 10^7$ Da, but are released on the endothelial cell surface as larger fibrils[35] that are rapidly cleaved by the a disintegrin and metalloproteinase with thrombospondin motif 13 metalloproteinase (ADAMTS13).[36] Plasma VWF can self-associate into multimers by shear-dependent[37] or -independent processes[38] and contains binding sites for adhesion receptors and extracellular matrix components. Platelet adhesion and aggregation are mediated by coordinated shear- and activation-dependent binding of platelet GPIbα to the VWF A1 domain[39] and integrin $\alpha_{IIb}\beta_3$ to the Arg-Gly-Asp (RGD) sequence[40] in the VWF C4 domain, respectively.[41-44]

In this article, we identify an unexpected link by which gut microbiota promote arterial thrombus formation through TLR2-dependent regulation of endothelial VWF synthesis in the liver endothelium.

Methods

Materials

Details on the sources of reagents, primer sequence, and mouse strains are given in the supplemental Experimental Procedures, available on the *Blood* Web site.

Mouse common carotid artery thrombosis model

Carotid injury was induced in anesthetized mice as previously described.[45] Briefly, a polyethylene catheter (0.28 mm interior diameter, 0.61 mm outside diameter; Smiths Medical Deutschland, Grasbrunn, Germany) was implanted into the right jugular vein. The left common carotid artery was dissected free and ligated vigorously (7.0 monofilament polypropylene, Prolene; Ethicon, Norderstedt, Germany) near the carotid bifurcation for 5 minutes to induce vascular injury. Before and after vascular injury, the fluorescent platelets were visualized in situ by in vivo epifluorescence high-speed video microscopy of the left common carotid artery. Mice with bleedings or any injury of the carotid artery during surgery were excluded from further analysis. There was no difference in the exclusion rate across the different experimental groups. All experiments were performed between 7 AM and 8 PM Mice were humanely sacrificed in end-point experiments 30 min after ligation of the carotid artery. All groups of mice were sex-, age-, and weight-matched and were free of clinical symptoms. All procedures performed on mice were approved by the local committee on legislation on protection of animals (Landesuntersuchungsamt Rheinland-Pfalz, Koblenz, Germany; 23177-07/G11-1-018, 23177-07/G13-1-072, 23177-07/G11-1-045, and 23177-07/G16-1-013).

Intravital high-speed video epifluorescence microscopy

Measurements were performed with a high-speed wide-field Olympus BX51WI fluorescence microscope by using a long-distance condenser and a ×10 (0.3 numerical aperture) water immersion objective with a monochromator (MT 20E; Olympus Deutschland, Hamburg, Germany) and a charge-coupled device camera (ORCA-R2; Hamamatsu Photonics, Hamamatsu, Japan). For image acquisition and analysis, the real-time imaging system Xcellence RT (Olympus Deutschland) software was used. Cell recruitment was quantified in 1 field of view (100 μm × 150 μm) of the injury area. Adherent cells were defined as cells or aggregates that did not move or detach from the endothelial lining within an observation period of 20 seconds, and cell counts are presented per millimeter squared.

Static platelet aggregate formation on laminin and adhesion assays

Laminin-coated coverslips were purchased from Neuvitro (El Monte, CA). Glass coverslips were degreased with 2 M hydrogen chloride in 50% ethanol for

30 minutes and coated with human VWF (Wilfactin, 12 IU/mL) or fibrinogen (200 μg/mL) overnight at 4°C and blocked with 1% bovine serum albumin for 1 hour at room temperature (RT). Washed mouse platelets were added after preparation and 5-(and 6) carboxy-2′,7′-dichlorofluorescein diacetate (DCF) or Rhodamin B staining to the coverslips for 60 minutes at RT in the dark. Where specified, stained, washed mouse platelets were incubated for 30 minutes in 200 μL of the indicated plasma sources or the indicated substances: human VWF Wilfactin (51 mIU/mL); anti-human VWF RGD sequence-specific monoclonal antibody LJ-152B-6 (5 μg/mL)[43]; and anti-α6 (GoH3) (10 μg/mL). The suspension was washed again and added to the coverslips for 60 minutes at RT in the dark. Where specified, Wilfactin-coated coverslips were preincubated with the anti-human VWF RGD monoclonal antibody[43] for 60 minutes. Prostaglandin E1 (Sigma-Aldrich, Taufkirchen, Germany) was used throughout all washing and adhesion steps at a concentration of 7.5 μM. For removal of unbound platelets, coverslips were washed with phosphate-buffered saline (pH 7.4), and matrix-bound platelets were visualized with the Olympus epifluorescence microscope BX51WI. Four images were chosen at random per experiment, and the percentage of covered surface area was quantified. For image acquisition and analysis, the real-time imaging system Xcellence RT (Olympus Deutschland) software was used.

Statistical analysis

Data are presented as the mean ± the standard error of the mean (SEM) and were analyzed with GraphPad Prism 5 software (GraphPad Software, San Diego, CA) by using the independent samples Student *t* test or Mann-Whitney test to compare 2 groups and analysis of variance (ANOVA) with the Tukey post hoc test; repeated measurement ANOVA (mixed model) or the Kruskal-Wallis test was used for >2 groups.

Results

Germ-free mice show impaired platelet thrombus growth at the injured carotid artery

We compared conventionally raised (CONV-R) and germ-free (GF) C57BL/6 mice in the arterial injury model induced by transient ligation of the common carotid artery.[45] Vascular injury in this model was restricted to a defined area where platelets adhere and aggregate on the exposed subendothelial matrix. Initial adhesion and thrombus formation was not significantly different in CONV-R and GF mice, but progressive platelet accumulation at the injury site was significantly less in GF mice (Figure 1A). Platelet counts and collagen-induced platelet aggregation in platelet-rich plasma were not different between GF mice and CONV-R controls (supplemental Figure 1A-B).

Plasma VWF is required for normal platelet adhesion/aggregation on extracellular matrix components under arterial flow conditions.[31] As a possible explanation for reduced thrombus growth, we found lower levels of VWF in the plasma of GF mice compared with CONV-R wild-type (WT) mice (Figure 1B). This was accompanied by reduced factor VIII (FVIII) antigen levels in plasma (Figure 1C). VWF multimer patterns (supplemental Figure 1C) and ADAMTS13 antigen levels (Figure 1D) were unchanged. Endothelial cells in lung[46] and liver microvasculature,[47] as well as megakaryocytes,[48] are known sites of VWF synthesis. VWF transcripts were reduced in the livers and bone marrow of GF mice compared with CONV-R WT mice, but not in the lungs (Figure 1E) and the carotid artery (supplemental Figure 1D). However, reduced VWF transcripts in the bone marrow of GF mice did not translate into reduced platelet VWF content (supplemental Figure 1E). Because FVIII transcripts were unchanged in the livers of GF vs CONV-R mice (Figure 1F), the reduced FVIII plasma levels
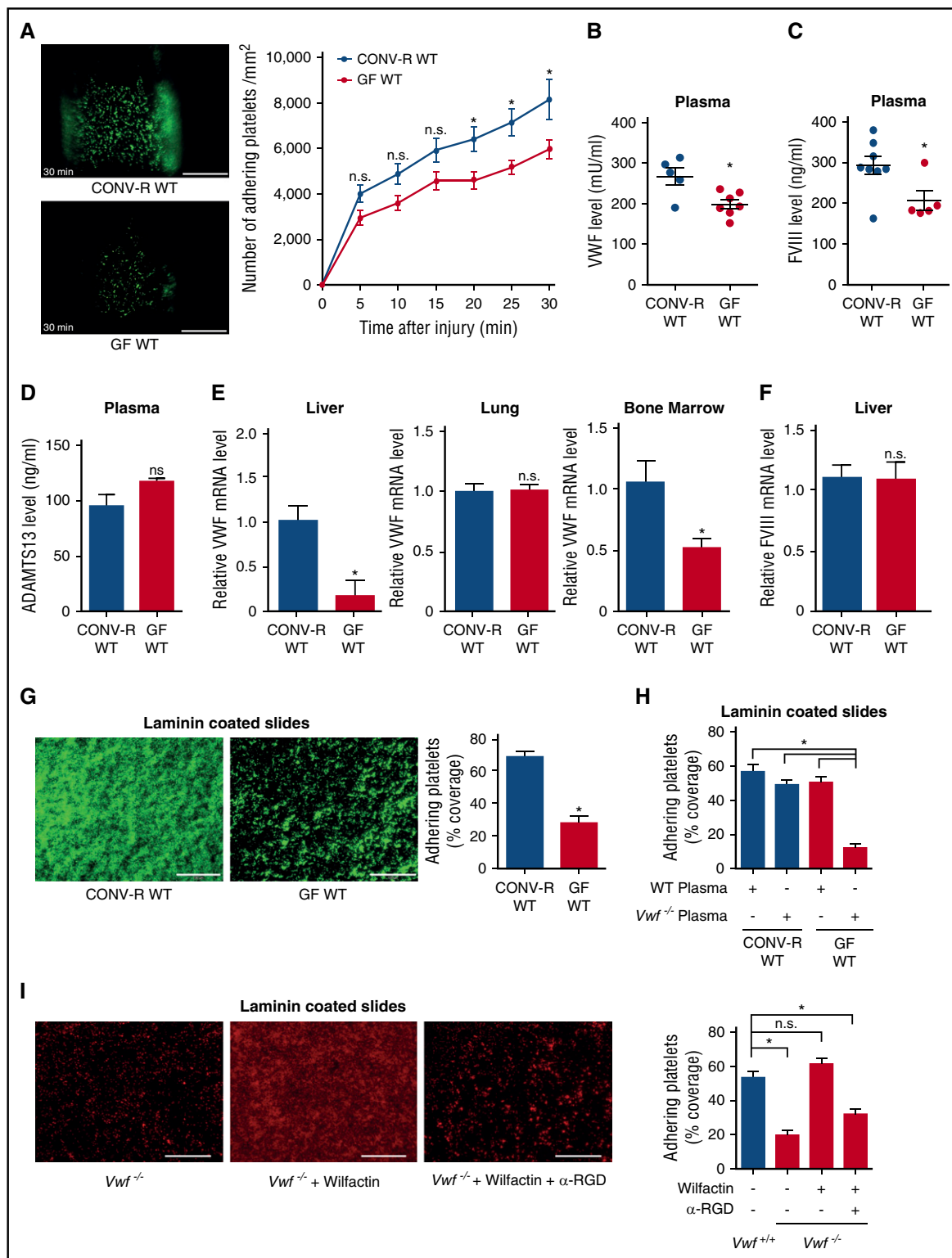
Figure 1. Reduced plasmatic VWF levels, hepatic synthesis, and platelet deposition in GF C57BL/6 mice. (A) Deposition of DCF, 5- (and 6) carboxy-2′,7′-dichlorofluorescein diacetate (carboxy-DCFDA)-stained platelets (green) to the ligation-injured common carotid artery in CONV-R WT (top) and GF WT mice (bottom) 30 minutes after transient ligation. Images of representative experiments are shown. Scale bar, 200 μm (10 mice per group). (B) VWF levels in PPP of CONV-R WT and GF WT mice (5-7 mice per group). (C) FVIII levels in PPP of CONV-R WT and GF WT mice (5-8 mice per group). (D) ADAMTS13 levels in plasma of CONV-R WT and GF WT mice (3 mice per group). (E) Relative VWF mRNA expression in the livers (4-5 mice per group), lungs (6 mice per group), and bone marrow (5 mice per group) of CONV-R WT compared with GF WT mice. (F) Relative FVIII mRNA expression in the liver (7 mice per group). (G) Deposition of DCF-stained, washed platelets (green) from CONV-R WT or GF WT mice to laminin. Representative images, scale bar, 100 μm; quadruplicate determination (4 mice per group). (H) Deposition of washed platelets from CONV-R WT and GF WT mice to laminin after 30 minutes of incubation with WT or $Vwf^{-/-}$ plasma; quadruplicate measurements (4 mice per group). (I) Deposition of washed platelets from $Vwf^{+/+}$ and homozygous $Vwf^{-/-}$ mice to laminin after 30 minutes of incubation with Wilfactin ± α-RGD; quadruplicate determination (4 mice per group); scale bar, 100 μm. Mean ± SEM, repeated measurement ANOVA (mixed model); independent-sample Student t tests or ANOVA with Tukey post hoc test, *P < .05. n.s., not significant.

likely result from reduced VWF-dependent stabilization of FVIII in plasma.

Reduced VWF plasma levels in GF mice did not result from increased VWF clearance rates, because injection of human VWF (Wilfactin) into GF and CONV-R mice did not reveal differences in VWF plasma clearance after 1 hour and 6 hours (supplemental Figure 1F). Differences in VWF clearance were further excluded by determination of the VWF-propeptide/VWF-antigen ratio (supplemental Figure 1G).[49] Because endothelial cell–derived plasma VWF is crucial for ferric chloride–induced carotid artery thrombosis,[34] we hypothesized that decreased VWF synthesis in the liver endothelium caused the smaller thrombus size after arterial injury in GF mice. Accordingly, we found that heterozygous $Vwf^{+/-}$ mice, with plasma VWF levels 50% lower than littermate $Vwf^{+/+}$ controls, exhibited reduced platelet accumulation on the ligation-injured carotid artery wall (supplemental Figure 2A).

We then used a no-flow ex vivo assay and found that platelets isolated from GF mice exhibited lower aggregate formation than platelets from CONV-R controls on immobilized laminin, a matrix component known to interact with VWF (Figure 1G). However, after washed GF platelets were exposed to WT, but not $Vwf^{-/-}$ platelet-poor plasma (PPP), their ability to adhere/aggregate on laminin was comparable to that of similarly treated CONV-R platelets (Figure 1H). Inhibiting activation with prostaglandin E1 markedly impaired platelet accumulation on laminin and the observed rescue of GF platelets exposed to normal plasma (supplemental Figure 2B). As previously documented under static[50] as well as flow conditions,[30,31,51] such an effect of prostaglandin E1 implies a role of VWF interaction with platelet $\alpha_{IIb}\beta_3$ in thrombus growth. In contrast, the presence of hirudin did not reduce adhesion of WT platelets (supplemental Figure 2B), demonstrating that activation was not dependent on thrombin generation.

To test the role of the VWF RGD motif, we incubated platelets from $Vwf^{-/-}$ mice with human VWF (Wilfactin) and demonstrated the recovery of markedly decreased laminin coverage to levels seen in WT controls (Figure 1I). This effect was prevented by the monoclonal antibody LJ-152B6 selectively blocking the RGD integrin binding site in the human VWF C4 domain.[43,44] Collectively, our results show that absence of the commensal microbiota impairs VWF synthesis in the liver, resulting in reduced platelet function involving VWF interaction with integrin $\alpha_{IIb}\beta_3$.

TLR2 specifically regulates expression of VWF in liver endothelial cells

Gut bacterial products trigger innate immune signaling and alter cellular immune homeostasis in the host,[1,4,5] but also reach the portal circulation and induce remote effects.[2,3] To identify a potential signaling pathway responsible for the regulation of hepatic VWF expression, we evaluated VWF messenger RNA (mRNA) levels in the livers and the lungs of $Tlr2^{-/-}$ and $Tlr4^{-/-}$ mice. Importantly, we found that VWF transcripts were reduced specifically in the livers, but were unchanged in the lungs of $Tlr2^{-/-}$ mice (Figure 2A). No changes in VWF expression were seen in $Tlr4^{-/-}$ mice compared with WT mice.

In line with our observation of reduced VWF levels in GF mice (Figure 1B), VWF plasma levels were reduced by 30% in $Tlr2^{-/-}$ mice compared with WT controls (Figure 2B). As found in GF mice, the reduced VWF plasma levels of $Tlr2^{-/-}$ mice could not be explained by differences in VWF clearance (supplemental Figure 3A-B). There were no apparent alterations in VWF multimer composition (Figure 2C),[36] an important determinant for platelet adhesion.[52] Furthermore, plasma levels of ADAMTS13, which is expressed in stellate cells in the liver

and considered the major regulator of VWF multimer size,[53] were unchanged (supplemental Figure 3C).

To show the precise location of liver synthesis of VWF, we isolated primary liver endothelial cells that also synthesize the antihemophilic cofactor FVIII. Although FVIII liver endothelial cell transcripts (Figure 2D) and plasma FVIII antigen levels (supplemental Figure 3D) were unchanged, VWF liver endothelial cell transcript levels were markedly reduced in $Tlr2^{-/-}$ mice compared with WT controls (Figure 2E). These differences in VWF transcript levels were not due to differences in vascularization, because PECAM-1 expression in the liver did not show changes in the hepatic microvasculature (supplemental Figure 3E-F).

We next analyzed whether the reduced VWF levels in $Tlr2^{-/-}$ mice result in diminished platelet deposition. Similar to GF platelets, $Tlr2^{-/-}$ platelets showed defective deposition on laminin (Figure 2F), but not the fibrinogen matrix (supplemental Figure 4A). Importantly, incubation with WT plasma restored $Tlr2^{-/-}$ platelet deposition on laminin (Figure 2F). Control experiments excluded that platelet TLR2 regulated the laminin-binding integrin α_6 (supplemental Figure 4B).[54] Thus, VWF synthesis in the liver and plasma levels are regulated by TLR2 and are a critical determinant for platelet deposition in this static assay.

Moderate changes in VWF influence platelet deposition on the extracellular matrix

We further characterized the effects of varying VWF levels on $Tlr2^{-/-}$ platelets in vitro. VWF levels in washed $Tlr2^{-/-}$ platelets were increased after 30 minutes of incubation with WT plasma, but were unchanged in WT platelets subjected to the same procedure, indicating an association of plasma VWF with $Tlr2^{-/-}$ platelets (Figure 3A). Importantly, incubation of $Tlr2^{-/-}$ platelets with $Vwf^{+/-}$ plasma was insufficient to recover platelet deposition on laminin, as seen on exposure to WT plasma (Figure 3B). Conversely, the incubation of $Vwf^{+/-}$ platelets with $Tlr2^{-/-}$ plasma also did not promote increased platelet deposition (data not shown), demonstrating that $Vwf^{+/-}$ and $Tlr2^{-/-}$ mice are defective in a common factor in their plasma.

Incubation of $Tlr2^{-/-}$ platelets with purified VWF, to achieve an estimated 30% increase in total VWF levels, increased platelet deposition on laminin that was prevented by the monoclonal antibody LJ-152B6 blocking the RGD integrin binding site of human VWF (Figure 3C), demonstrating rescue of matrix interaction by VWF interacting with platelet integrins. This conclusion was further substantiated by platelet adhesion studies to immobilized VWF that, under our experimental conditions, was sensitive to antibody blockade of the VWF integrin binding site (Figure 3D). Intriguingly, $Tlr2^{-/-}$ platelets and platelets isolated from $Vwf^{-/-}$ mice showed reduced deposition to surface-coated VWF as compared with platelets from WT controls, but preincubation of $Tlr2^{-/-}$ or $Vwf^{-/-}$ platelets with WT plasma fully restored defective deposition. Blockade of the human VWF RGD integrin binding site with the antibody LJ-152B-6[43,44] prevented plasma exposure–stimulated adhesion of both knockout platelets, further confirming the common defect in the plasma leading to defective matrix interaction of platelets. Thus, reduced plasma VWF levels in GF and $Tlr2^{-/-}$ mice diminish platelet integrin reactivity with VWF.

Thrombus growth in *Tlr2*-deficient mice is dependent on the plasma milieu

Consistent with the reduced VWF levels, CONV-R $Tlr2^{-/-}$ mice showed decreased platelet thrombus growth in the carotid artery ligation model (Figure 4A; supplemental Videos 1 and 2). Importantly,
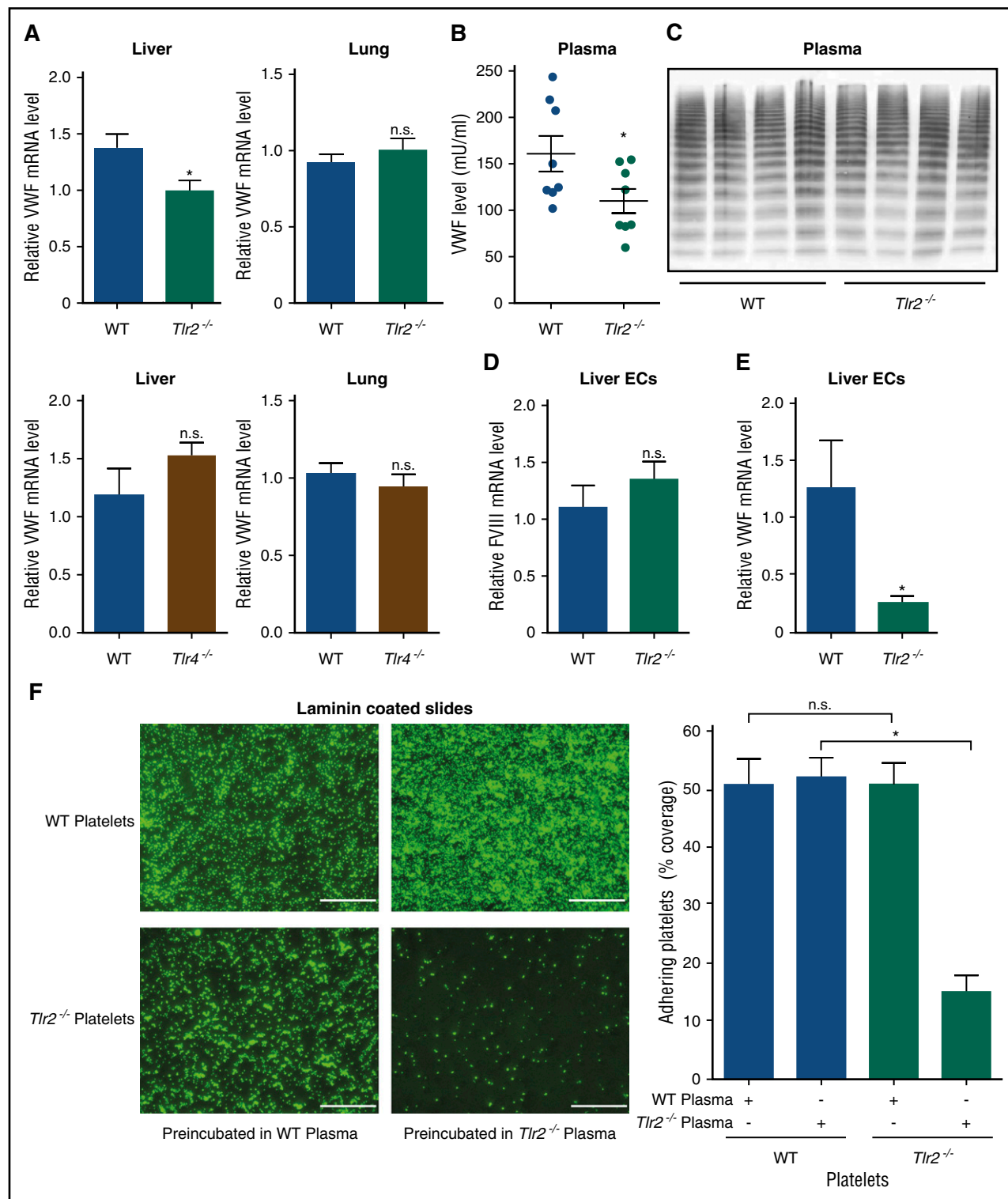
Figure 2. Impaired deposition of *Tlr2*-deficient platelets to laminin coatings is dependent on reduced plasma VWF levels and hepatic VWF synthesis in *Tlr2*^−/− C57BL/6 mice. (A) Relative VWF mRNA expression in the livers and lungs of WT, *Tlr2*^−/−, and *Tlr4*^−/− mice (7-9 mice per group). (B) VWF level in PPP of WT and *Tlr2*^−/− mice (8 mice per group). (C) VWF multimer composition in PPP of WT and *Tlr2*^−/− mice (4 mice per group). (D) FVIII mRNA levels in primary mouse liver endothelial cells of WT and *Tlr2*^−/− mice (5 mice per group). (E) VWF mRNA levels in primary mouse liver endothelial cells of WT and *Tlr2*^−/− mice (5 mice per group). (F) Static laminin deposition of DCF-stained, washed platelets (green) of WT or *Tlr2*^−/− mice after 30 minutes of incubation with WT or *Tlr2*^−/− plasma. Representative images (left) and quantification (right); quadruplicate measurements (3 mice per group). Scale bar, 100 μm; mean ± SEM; independent-sample Student *t* tests or ANOVA with Tukey post hoc test or Kruskal-Wallis test, *$P < .05$. EC, endothelial cell; n.s., not significant.

platelet deposition did not differ at early time points (5 minutes) (Figure 4B). We performed a series of control experiments to identify alternative explanations for the reduced platelet thrombus formation.

Evaluation of VWF expression in sham-operated and ligation-injured carotid arteries was indistinguishable between CONV-R WT and CONV-R *Tlr2*^−/− mice (supplemental Figure 5A-B). Furthermore,
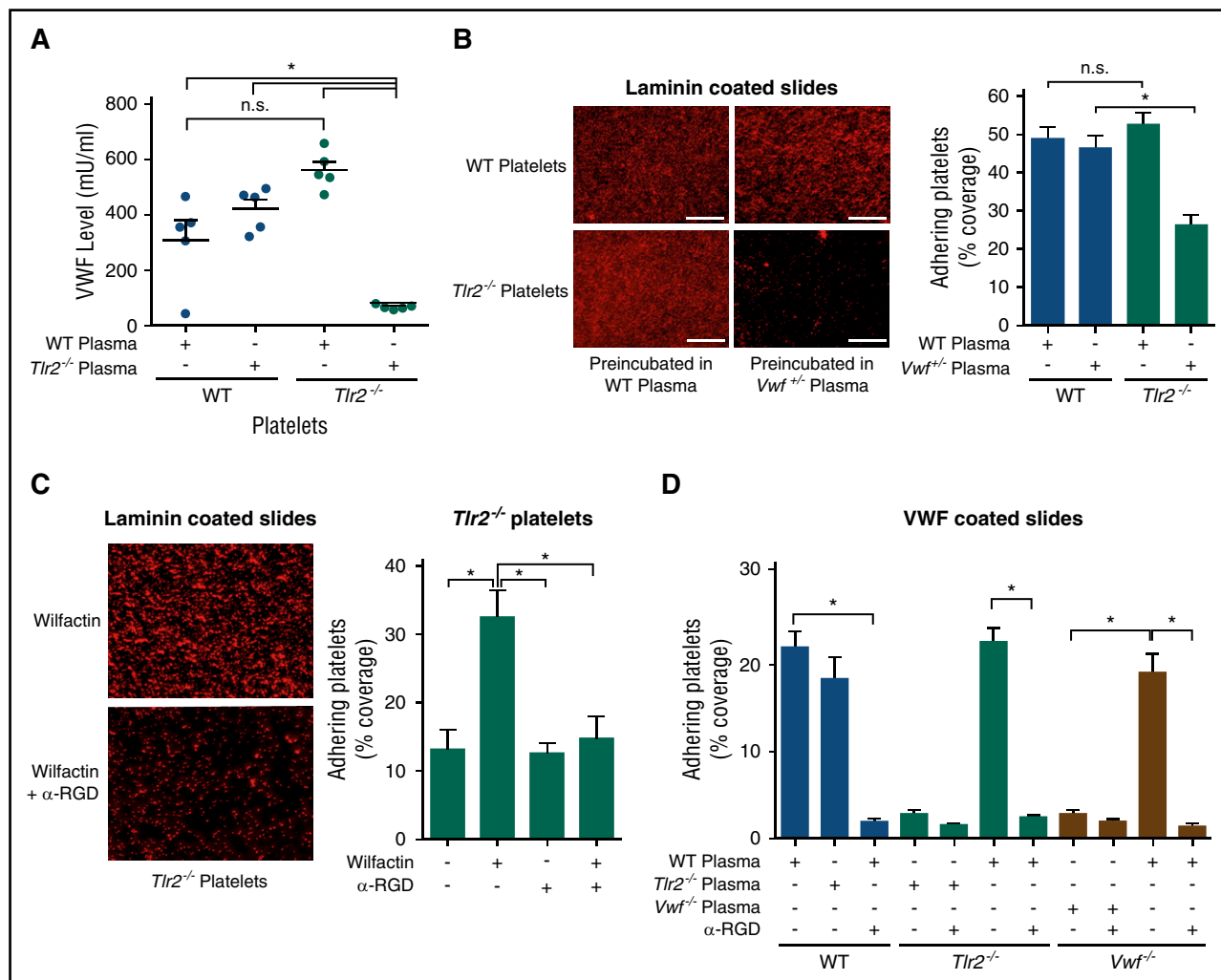
Figure 3. Plasma VWF levels determine platelet deposition on laminin and VWF coatings. (A) VWF concentration of WT or $Tlr2^{-/-}$ platelet lysates after incubation with the indicated plasmas (5 mice per group). (B) Static laminin deposition of Rhodamin B–stained, washed WT and $Tlr2^{-/-}$ platelets (red) after 30 minutes of preincubation with WT ($Vwf^{+/+}$) or $Vwf^{+/-}$ plasma. Representative images (left) and quantification (right); quadruplicate determination (3 mice per group). Representative images are shown. (C) Laminin adhesion of washed $Tlr2^{-/-}$ platelets supplemented with 51 mIU/mL of human VWF (Wilfactin) in the absence or presence of anti-VWF LJ-152B-6 (α-RGD) directed against the RGD motif; quadruplicate determination (3 mice per group). (D) Deposition of washed platelets from WT, $Tlr2^{-/-}$, or $Vwf^{-/-}$ mice preincubated for 30 minutes with the indicated plasma sources on human VWF coatings. Anti-VWF LJ-152B-6 (α-RGD) was added where indicated. Quadruplicate determination (3 mice per group). Scale bar, 100 μm; mean ± SEM; independent-sample Student t tests or ANOVA with Tukey post hoc test or Kruskal-Wallis test, *$P < .05$. n.s., not significant.

Weibel Palade body secretion was apparently not affected in $Tlr2^{-/-}$ and GF mice, because plasma levels of soluble P-selectin were unchanged (supplemental Figure 5C-D). We also analyzed whether Kupffer cells, the major cell type involved in VWF clearance in the liver,[55] were influenced by $Tlr2$ deficiency. By immunohistochemistry (supplemental Figure 6A), the numbers of CD68^{+} Kupffer cells were unchanged in $Tlr2^{-/-}$ mice compared with WT controls, irrespective of whether the carotid artery was ligated or not. Thus, increased VWF clearance by Kupffer cells was an unlikely cause for decreased VWF plasma levels in $Tlr2^{-/-}$ mice and for the changes in thrombus growth.

Confirming the integrity of the intestinal barrier during experimental procedures, no bacterial 16S ribosomal DNA could be amplified from the livers of sham-operated or ligated WT and $Tlr2^{-/-}$ mice (supplemental Figure 6B). Chronic liver damage of $Tlr2^{-/-}$ versus WT mice was excluded by quantification of aspartate aminotransferase activity (supplemental Figure 6C). Furthermore, hepatic inflammation of $Tlr2^{-/-}$ versus WT mice was excluded by quantifying mRNA expression levels of tumor necrosis factor-α (supplemental Figure 6D).

In addition, leukocyte deposition at the vascular injury site was a rare event (supplemental Figure 6E), supporting the overall conclusion that TLR2 primarily influences plasma composition and the interaction of VWF with platelets. Additional control experiments addressed the function of $Tlr2$-deficient platelets. $Tlr2$ deficiency had no effect on platelet counts, tail bleeding time, platelet volume, granularity, shape, or white blood cell counts (supplemental Figure 6F-K). A platelet autonomous signaling defect was also unlikely because of unaltered platelet agonist responses of $Tlr2^{-/-}$ platelets compared with WT control platelets (supplemental Figure 7A-H).

To further exclude that the reduced platelet thrombus growth observed in $Tlr2^{-/-}$ mice was caused by platelet TLR2 signaling, we reconstituted platelet-depleted WT mice with $Tlr2^{-/-}$ platelets. We used human GPIbα-transgenic mice that were depleted with an anti-human GPIbα antibody nonreactive with mouse GPIbα.[56] Depleted mice were reconstituted with platelets from WT or $Tlr2^{-/-}$ mice and analyzed for thrombus formation in the ligation injury model. Consistent with the normalization of defective adhesion by WT
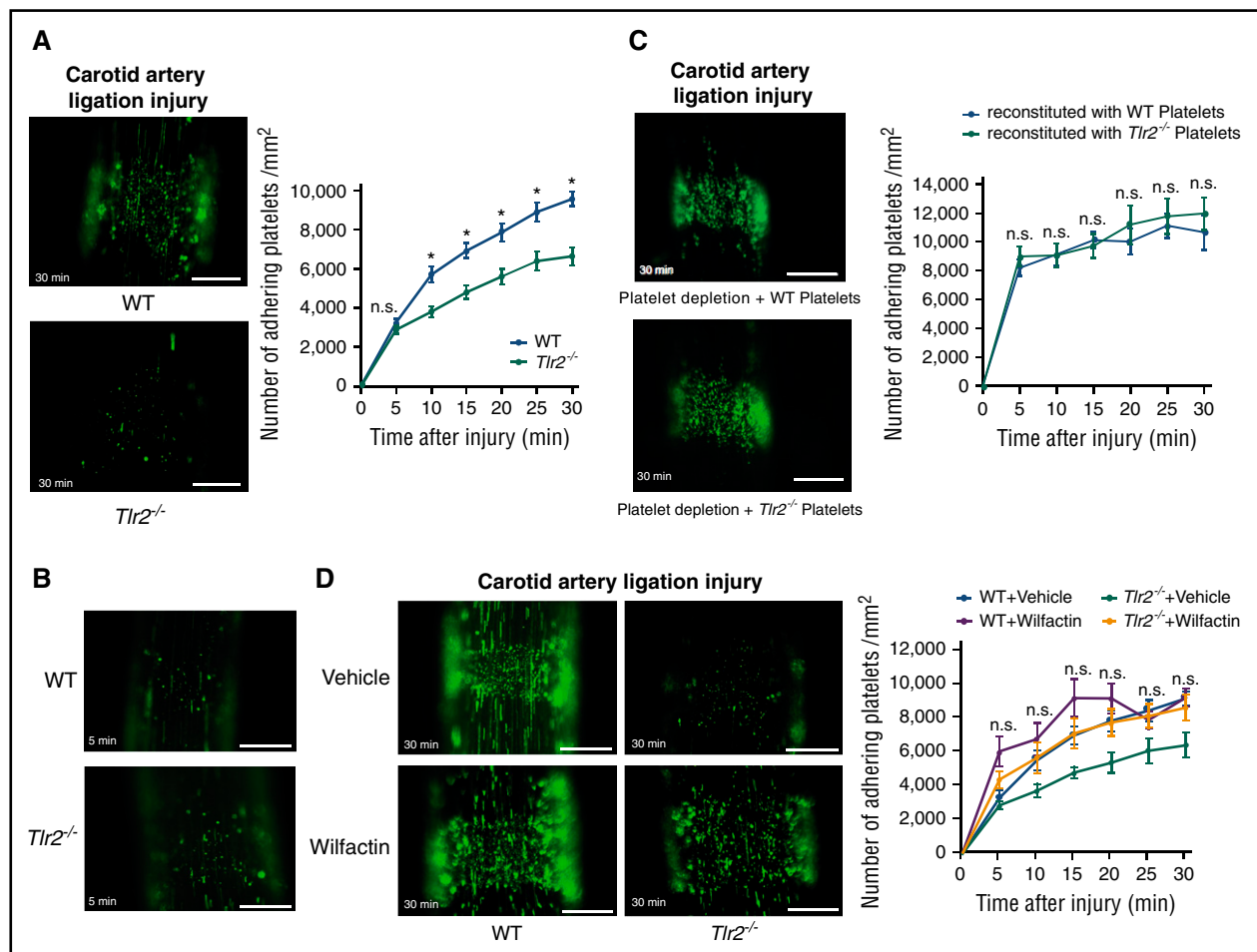
Figure 4. Reduced platelet deposition to the ligation injured carotid artery in *Tlr2*-deficient mice is independent of the platelet genotype, and the adhesion defect is rescued by VWF supplementation. (A) Imaging of DCF, 5- (and 6) carboxy-2',7'-dichlorofluorescein diacetate (carboxy-DCFDA)-stained platelet deposits (green) to the ligation-injured common carotid artery in WT (top) and *Tlr2*−/− (bottom) mice 30 minutes after transient ligation; representative images and quantification (8-11 mice per group). (B) Representative images of DCF-stained platelet deposits (green) to the ligation-injured common carotid artery in WT (top) and *Tlr2*−/− (bottom) mice 5 minutes after transient ligation. (C) Platelet deposition in hGPIbα mice after platelet depletion and reconstitution with DCF stained WT (top) or *Tlr2*−/− platelets (bottom) 30 minutes after transient ligation; representative images and quantification (10 mice per group). (D) Imaging of DCF-stained platelet deposits (green) to the ligation-injured common carotid artery in WT and *Tlr2*−/− mice treated with sodium chloride (vehicle) or 153 mIU human VWF (Wilfactin) per mouse (6-10 mice per group). Scale bar, 200 μm. Representative images are shown. Mean ± SEM; repeated measurement ANOVA (mixed model), *$P < .05$. n.s., not significant.

plasma exposure in vitro, the number of *Tlr2*−/− platelets deposited at the injury site was indistinguishable from WT platelets after infusion into WT blood (Figure 4C).

To confirm in vivo that a quantitative deficiency of VWF was responsible for reduced platelet deposition in *Tlr2*−/− mice after carotid artery ligation injury, we increased VWF plasma levels by a calculated 30% through infusion of VWF. Supplementation of VWF increased platelet deposition in *Tlr2*−/− mice to levels seen in WT mice (Figure 4D). Therefore, our results support the conclusion that the moderate quantitative differences in plasma VWF between WT and *Tlr2*−/− mice influence VWF interaction with platelets and that VWF was the primary determinant for reduced thrombus formation of *Tlr2*−/− platelets at sites of vessel injury.

The commensal gut microbiota regulate plasma VWF levels through TLR2

To confirm that the thrombosis phenotype of *Tlr2*−/− mice was due to microbial colonization, we rederived GF *Tlr2*−/− mice by aseptic hysterectomy. To exclude genetic drift, *Tlr2*−/− and WT mice were crossed under GF conditions, and littermates from heterozygous breeding were

compared. The reduction in VWF plasma levels and hepatic VWF transcripts seen in conventionally raised *Tlr2*−/− mice (Figure 2A-B) were no longer observed in GF *Tlr2*−/− mice compared with GF WT mice (Figure 5A,C). Accordingly, VWF multimers and VWF mRNA levels in liver and lung tissue were indistinguishable between WT and *Tlr2*−/− mice under GF conditions (Figure 5B-C). Importantly, the marked difference in platelet deposition at the carotid artery ligation injury site observed between WT and *Tlr2*−/− mice under CONV-R conditions was no longer seen in littermates of GF WT and GF *Tlr2*−/− mice (Figure 5D; supplemental Videos 3 and 4).

Colonization of GF WT and GF *Tlr2*−/− mice restores differences in platelet deposition

Next, we recolonized strain-matched GF *Tlr2*−/− and GF *Tlr2*+/+ mice with cecal microbiota from CONV-R donor mice and analyzed litters from recolonized mice in the carotid artery ligation injury model. Confirming the involvement of gut microbial communities, conventional-derived (CONV-D) progeny showed that colonization was sufficient to restore the platelet deposition differences between *Tlr2*−/− mice and WT controls in vivo (Figure 6A).

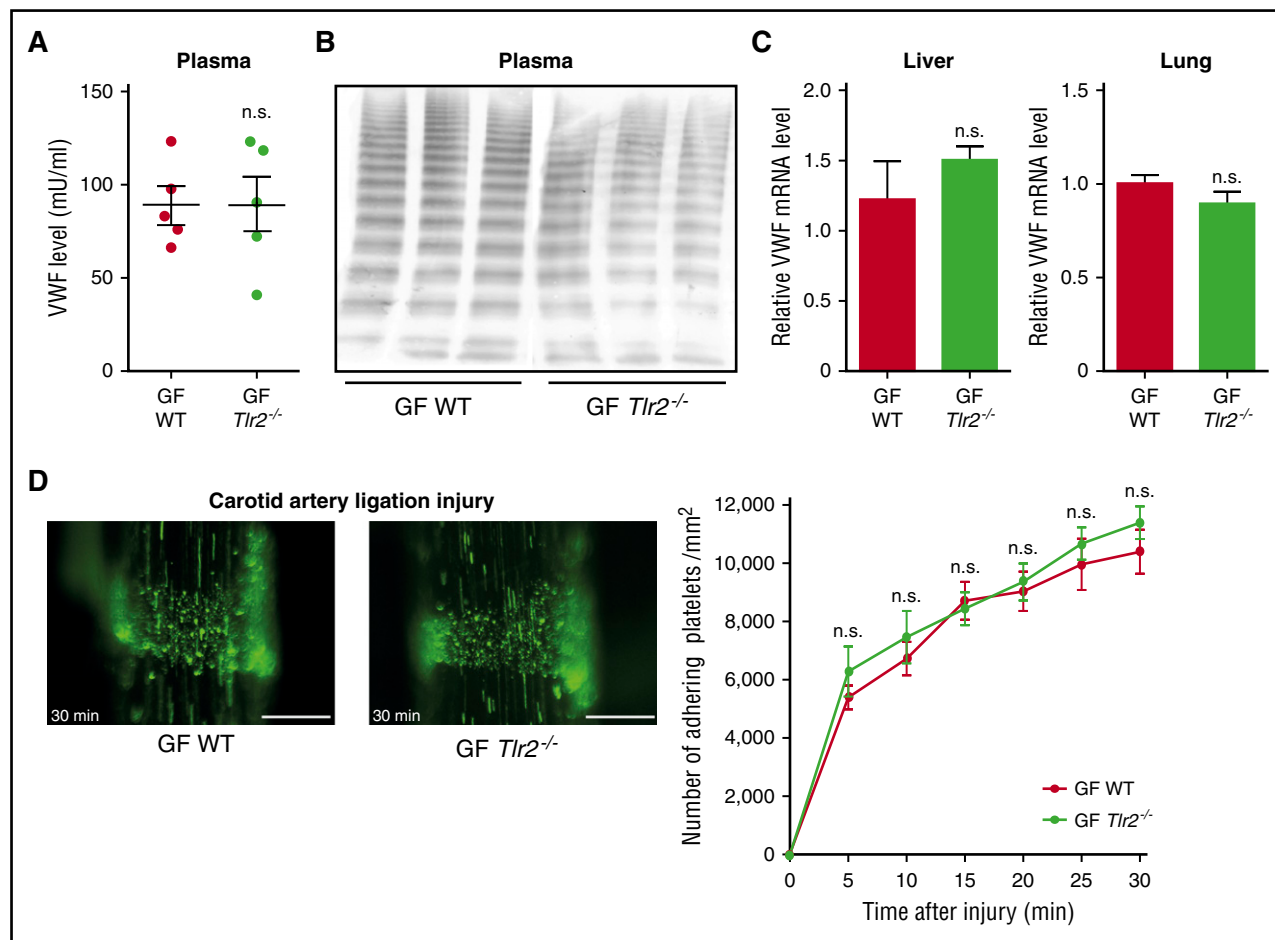**Figure 5. The platelet deposition defect of *Tlr2*$^{-/-}$ mice is microbiota dependent.** (A) VWF level in PPP of GF WT compared with GF *Tlr2*$^{-/-}$ mice (5 mice per group). (B) VWF multimer composition in PPP from GF WT and GF *Tlr2*$^{-/-}$ mice (3 mice per group). (C) VWF mRNA expression in the livers (7 mice per group) and the lungs (7 mice per group) of GF WT and GF *Tlr2*$^{-/-}$ mice. (D) Deposition of DCF, 5- (and 6) carboxy-2',7'-dichlorofluorescein diacetate (carboxy-DCFDA)-stained platelets (green) to the ligation-injured common carotid artery in GF WT (left) or GF *Tlr2*$^{-/-}$ (right) mice 30 minutes after transient ligation (7-9 mice per group). Scale bar, 200 μm. Mean ± SEM; independent-sample Student *t* tests or repeated measurement ANOVA (mixed model). n.s., not significant.

We confirmed in a series of independent experiments that recolonization was sufficient to restore the difference in reactivity of WT versus *Tlr2*$^{-/-}$ platelets. GF *Tlr2*$^{+/+}$ and GF *Tlr2*$^{-/-}$ littermates from several pregnancies were colonized with microbiota from the same CONV-R WT donor mouse at weaning for 4 weeks and then analyzed for platelet interaction with the extracellular matrix in vitro (Figure 6B). Importantly, a consistent difference in platelet deposition was restored, and hepatic VWF transcript levels were increased in the same colonized *Tlr2*$^{+/+}$ mice compared with colonized *Tlr2*$^{-/-}$ littermates (Figure 6C).

We further analyzed the intestinal microbiome of these conventionalized mice and found that community diversity and composition in the gut lumen was largely unchanged between *Tlr2*$^{-/-}$ and WT mice (supplemental Figures 8A-F and 9A-D). Interestingly and in contrast, the *Tlr2* genotype does appear to influence the mucosa-associated microbial communities, which is consistent with previous hypotheses predicting a greater host genetic influence in the mucosa.[57] To directly test whether stimulation with bacterial ligands can augment endothelial VWF transcript levels, we treated cultured endothelial cells with PG. This increased VWF transcript levels (Figure 6D). We then fed GF WT mice the TLR2 agonist LTA in the drinking water under isolator conditions for 7 days. Indeed, providing this TLR2 agonist was sufficient to increase hepatic VWF expression under these conditions (Figure 6E),

demonstrating that TLR agonists derived from the gastrointestinal tract regulate hepatic VWF synthesis.

Discussion

The commensal microbiota are an environmental factor whose metabolic functions have been linked to cardiovascular disease,[14,58] the leading cause of morbidity and mortality in industrialized countries. Our study identifies a novel connection in which microbiota influence platelet function not directly, but indirectly through hepatic TLR2 signaling. The delineated innate immune signaling pathway links intestinal microbiota to liver endothelial function that fosters prothrombotic VWF-integrin interaction on platelets (Figure 7).

As shown in this study, microbiota modulate hepatic VWF expression and plasmatic VWF levels, a major risk factor of arterial thrombosis and stroke,[34,59,60] through TLR2. In heterozygous *Vwf*$^{+/-}$ mice, a 50% reduction in plasma VWF levels is sufficient to substantially reduce platelet deposition at arterial ligation injury sites. We find that diminished VWF plasma levels are decisive for reduced platelet deposition in GF and *Tlr2*$^{-/-}$ mice. Importantly, GF *Tlr2*$^{-/-}$ and GF WT mice were indistinguishable in VWF plasma levels, hepatic synthesis, and platelet
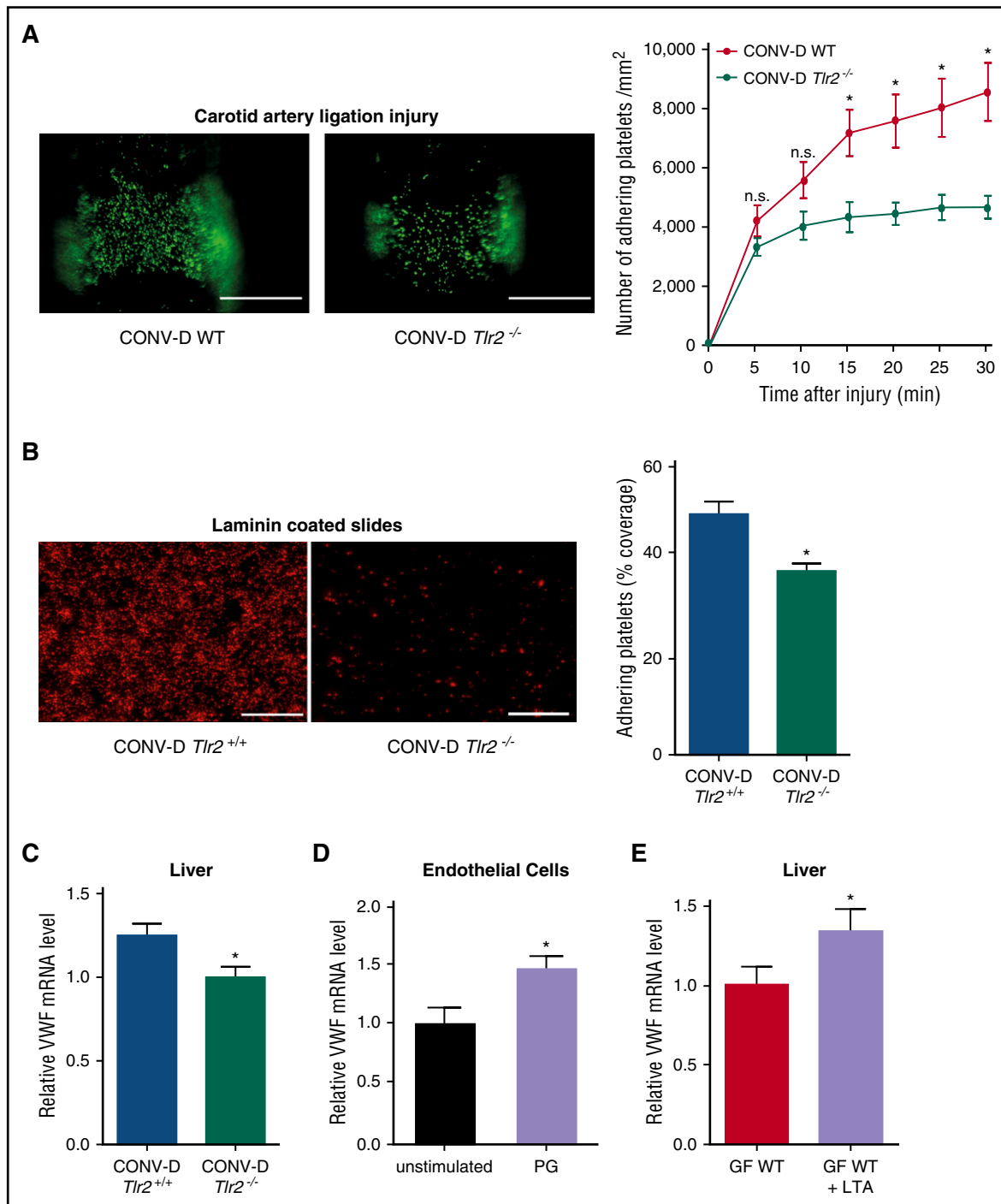
Figure 6. Impaired platelet deposition of colonized *Tlr2*^{−/−} mice is restored by colonization of GF WT and GF *Tlr2*^{−/−} mice. (A) Deposition of DCF, 5- (and 6) carboxy-2',7'-dichlorofluorescein diacetate (carboxy-DCFDA)-stained platelets (green) to the ligation-injured common carotid artery in CONV-D WT (left) or CONV-D *Tlr2*^{−/−} (right) mice 30 minutes after transient ligation (second generation offspring: mice were taken out from the germ-free environment and the second generation of these mice was analyzed; aged 8-14 weeks). Scale bar, 200 μm (8 mice per group). (B) Deposition of Rhodamin B–stained, washed platelets (red) from CONV-D WT (*Tlr2*^{+/+}) or CONV-D *Tlr2*^{−/−} mice to laminin. Representative images, scale bar, 100 μm; quadruplicate measurements (3 mice per group). (C) VWF mRNA expression in the livers of CONV-D WT (*Tlr2*^{+/+}) or CONV-D *Tlr2*^{−/−} mice (6-7 mice per group). (D) VWF mRNA expression of PG-stimulated (10 μg/mL, 2 h) HUVECs (N = 5-6 per group). (E) Hepatic VWF mRNA expression of GF C57BL/6 mice treated with lipoteichoic acid (LTA) (10 μg/mL) in drinking water for 7 days (6-7 mice per group). Mean ± SEM, independent-sample Student *t* tests or repeated measurement ANOVA (mixed model), *$P < .05$. n.s., not significant.

deposition to the ligation-injured carotid artery. Conventionalization of GF WT and GF *Tlr2*^{−/−} mice restored the differences in platelet deposition on matrix coatings in vitro and in the carotid artery ligation model. Colonization of GF littermates was sufficient to cause a difference in hepatic VWF expression between WT and *Tlr2*^{−/−} mice.

The gut metagenomes of patients with stenotic atherosclerotic plaques in the carotid artery are enriched in genes encoding the synthesis of the TLR2 agonist PG.[14] Microbiota-derived metabolites and nutrition are additional factors that affect experimental thrombus formation and thrombosis risk.[14,59,61] The gut commensal–derived
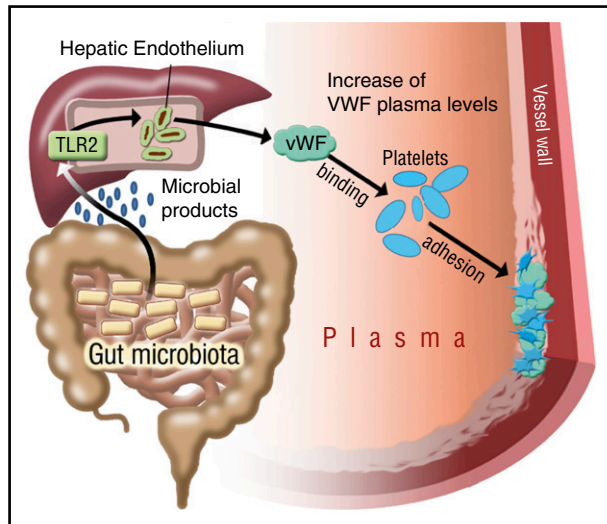
Figure 7. Illustration on the effect of gut microbiota on TLR2 signaling and VWF-mediated platelet deposition to the arterial injury site. Microbial patterns released by commensal microbiota augment VWF synthesis by triggering TLR2 signaling in the hepatic endothelium. In the absence of microbiota, reduced VWF plasma levels result in impaired VWF-integrin binding and reduced platelet deposition to the subendothelial matrix at the arterial injury site.

metabolite trimethylamine N-oxide or microbiota-triggered serotonin synthesis by colonic enterochromaffin cells were recently identified as regulators of platelet function.[61,62] Carboxyalkylpyrrole-phosphadidylethanolamine derivatives in hyperlipidemic atherosclerotic mice enhance platelet TLR2-induced thrombus formation,[21] and trimethylamine N-oxide, a commensal metabolite with increased synthesis under a choline-enriched diet, promotes ferric chloride–induced occlusive thrombus formation.[61] Because diets were strictly controlled in our experimental settings, the demonstrated role of commensal microbiota on platelet deposition to the carotid artery is notably independent of dietary intervention.

Under noninfectious conditions, intestinal gut microbes typically do not access the liver, but it has been demonstrated that fluorescein isothiocyanate-dextran of 4 kDa freely diffuses through the intestinal endothelial barrier[63] and that the hepatic endothelium is exposed to products of the commensal gut microbiota, triggering innate immune receptor signaling.[1-3] Because TLR2 agonists can induce canonical TLR signaling responses in platelets, we initially attributed the platelet adhesion defect of $Tlr2^{-/-}$ platelets to platelet autonomous signaling. However, extensive characterization in platelet function assays did not uncover abnormalities of $Tlr2^{-/-}$ platelets themselves, but rather of their ligand VWF. We show that delivery of the TLR2 agonist LTA via drinking water is sufficient to increase hepatic VWF transcript levels, supporting a role of gastrointestinal bacterial ligands in the regulation of hepatic VWF expression.

We propose that TLR2 acts as the key sensor for gut microbial ligands[1-3] that can induce remote signaling in the liver endothelium, thus leading to adaptive changes in plasmatic clotting factor levels after microbial colonization of the host. VWF and FVIII mRNA expression in endothelial cells varies strongly in different vascular beds, and the expression levels of these factors do not necessarily correlate with each other.[64] Although TLR2 signaling is known to promote Weibel-Palade body exocytosis and VWF release of aortic endothelial cells,[23] VWF mRNA and protein expression in the carotid arteries was unchanged in sham-operated or ligation-injured $Tlr2^{-/-}$ and GF mice, thus, excluding that altered VWF levels in the injured vessels caused the observed platelet

adhesion defect. Moreover, reduced VWF plasma levels in $Tlr2^{-/-}$ mice cannot be explained by altered Kupffer cell numbers in the liver, representing the primary clearance route of VWF,[55] or differences in VWF clearance. Altogether, our experiments demonstrate that decreased VWF plasma levels in $Tlr2^{-/-}$ mice are caused by decreased hepatic synthesis.

The synergistic engagement of redundant adhesion receptors for VWF mediated platelet deposition to the extracellular matrix is shear stress dependent.[31] Our results position the microbiota- and TLR2-dependent increase in plasma VWF and the effects on VWF binding to platelet integrins as central prothrombotic mechanisms that foster platelet thrombus growth after ligation injury of the carotid artery. Our finding of the prothrombotic role of the microbiota should foster translational research into the interdependence of VWF plasma levels and increased thrombosis risk.[34,59,60] It will be of interest to determine whether nutrition (eg, lipid-rich diets) combined with the metabolic function of the commensal gut microbiota[61,62] can impact the gut-vascular barrier,[63] affecting levels of bacterial TLR ligands in the portal circulation,[1-3] and thus amplify VWF synthesis in the liver endothelium and the risk for thrombosis. Our study demonstrates that the hepatic microvasculature is not only the site for the control of acute infection in immunothrombosis,[15,47] but is also a homeostatic regulator of plasma components that affect the reactivity of platelets and remote vascular thrombosis.

Authorship

Contribution: S.J. performed experiments, analyzed data, and contributed to writing the manuscript; K.K., M.L., T.H., A.K., B.K., N.H., C.R., S.S., E.W., K.E., P.R., S.H., and K.J. performed experiments and analyzed data; J.F.B., B.L., C.J.B., K.J., M.-L.v.B., Z.M.R., S.M., and U.W. provided expert technical advice and contributed to the design of the study; Z.M.R. contributed essential mice and reagents; W.R. designed and analyzed data and wrote the manuscript; and C.R. designed experiments, performed experiments, analyzed data, and wrote the manuscript.

Conflict-of-interest disclosure: The authors declare no competing financial interests.

ORCID profiles: S.J., 0000-0003-4680-7013; K.J., 0000-0001-5313-4035; C.R., 0000-0002-0696-2636.

Correspondence: Christoph Reinhardt, Center for Thrombosis and Hemostasis, University Medical Center, Johannes Gutenberg University of Mainz, Langenbeckstrasse 1, Building 403, 1st Floor, 55131 Mainz, Germany; e-mail: christoph.reinhardt@unimedizin-mainz.de

References

1. Clarke TB, Davis KM, Lysenko ES, Zhou AY, Yu Y, Weiser JN. Recognition of peptidoglycan from the microbiota by Nod1 enhances systemic innate immunity. *Nat Med*. 2010;16(2):228-231.

2. Cani PD, Amar J, Iglesias MA, et al. Metabolic endotoxemia initiates obesity and insulin resistance. *Diabetes*. 2007;56(7):1761-1772.

3. Balmer ML, Slack E, de Gottardi A, et al. The liver may act as a firewall mediating mutualism between the host and its gut commensal microbiota. *Sci Transl Med*. 2014;6(237):237ra66.

4. Round JL, Lee SM, Li J, et al. The Toll-like receptor 2 pathway establishes colonization by a commensal of the human microbiota. *Science*. 2011;332(6032):974-977.

5. Deshmukh HS, Liu Y, Menkiti OR, et al. The microbiota regulates neutrophil homeostasis and host resistance to *Escherichia coli* K1 sepsis in neonatal mice. *Nat Med*. 2014;20(5):524-530.

6. Kawai T, Akira S. The role of pattern-recognition receptors in innate immunity: update on Toll-like receptors. *Nat Immunol*. 2010;11(5):373-384.

7. Dauphinee SM, Karsan A. Lipopolysaccharide signaling in endothelial cells. *Lab Invest*. 2006; 86(1):9-22.

8. Dunzendorfer S, Lee HK, Tobias PS. Flow-dependent regulation of endothelial Toll-like receptor 2 expression through inhibition of SP1 activity. *Circ Res*. 2004;95(7):684-691.

9. Li J, Ma Z, Tang ZL, Stevens T, Pitt B, Li S. CpG DNA-mediated immune response in pulmonary endothelial cells. *Am J Physiol Lung Cell Mol Physiol*. 2004;287(3):L552-L558.

10. Andonegui G, Kerfoot SM, McNagny K, Ebbert KV, Patel KD, Kubes P. Platelets express functional Toll-like receptor-4. *Blood*. 2005; 106(7):2417-2423.

11. Aslam R, Speck ER, Kim M, et al. Platelet Toll-like receptor expression modulates lipopolysaccharide-induced thrombocytopenia and tumor necrosis factor-alpha production in vivo. *Blood*. 2006;107(2):637-641.

12. Shiraki R, Inoue N, Kawasaki S, et al. Expression of Toll-like receptors on human platelets. *Thromb Res*. 2004;113(6):379-385.

13. Panigrahi S, Ma Y, Hong L, et al. Engagement of platelet toll-like receptor 9 by novel endogenous ligands promotes platelet hyperreactivity and thrombosis. *Circ Res*. 2013;112(1):103-112.

14. Karlsson FH, Fåk F, Nookaew I, et al. Symptomatic atherosclerosis is associated with an altered gut metagenome. *Nat Commun*. 2012;3:1245.

15. Massberg S, Grahl L, von Bruehl ML, et al. Reciprocal coupling of coagulation and innate immunity via neutrophil serine proteases. *Nat Med*. 2010;16(8):887-896.

16. Semple JW, Italiano JE Jr, Freedman J. Platelets and the immune continuum. *Nat Rev Immunol*. 2011;11(4):264-274.

17. Semeraro F, Ammollo CT, Morrissey JH, et al. Extracellular histones promote thrombin generation through platelet-dependent mechanisms: involvement of platelet TLR2 and TLR4. *Blood*. 2011;118(7):1952-1961.

18. Rivadeneyra L, Carestia A, Etulain J, et al. Regulation of platelet responses triggered by Toll-like receptor 2 and 4 ligands is another non-genomic role of nuclear factor-kappaB. *Thromb Res*. 2014;133(2):235-243.

19. Blair P, Rex S, Vitseva O, et al. Stimulation of Toll-like receptor 2 in human platelets induces a thromboinflammatory response through activation of phosphoinositide 3-kinase. *Circ Res*. 2009; 104(3):346-354.

20. Rex S, Beaulieu LM, Perlman DH, et al. Immune versus thrombotic stimulation of platelets differentially regulates signalling pathways, intracellular protein-protein interactions, and alpha-granule release. *Thromb Haemost*. 2009; 102(1):97-110.

21. Biswas S, Xin L, Panigrahi S, et al. Novel phosphatidylethanolamine derivatives accumulate in circulation in hyperlipidemic ApoE⁻/⁻ mice and activate platelets via TLR2. *Blood*. 2016;127(21): 2618-2629.

22. Shin H-S, Xu F, Bagchi A, et al. Bacterial lipoprotein TLR2 agonists broadly modulate endothelial function and coagulation pathways in vitro and in vivo. *J Immunol*. 2011;186(2): 1119-1130.

23. Into T, Kanno Y, Dohkan J, et al. Pathogen recognition by Toll-like receptor 2 activates Weibel-Palade body exocytosis in human aortic endothelial cells. *J Biol Chem*. 2007;282(11): 8134-8141.

24. Denis C, Methia N, Frenette PS, et al. A mouse model of severe von Willebrand disease: defects in hemostasis and thrombosis. *Proc Natl Acad Sci USA*. 1998;95(16):9524-9529.

25. Brill A, Fuchs TA, Chauhan AK, et al. von Willebrand factor-mediated platelet adhesion is critical for deep vein thrombosis in mouse models. *Blood*. 2011;117(4):1400-1407.

26. Nightingale T, Cutler D. The secretion of von Willebrand factor from endothelial cells; an increasingly complicated story. *J Thromb Haemost*. 2013;11(suppl 1):192-201.

27. Wagner DD, Olmsted JB, Marder VJ. Immunolocalization of von Willebrand protein in Weibel-Palade bodies of human endothelial cells. *J Cell Biol*. 1982;95(1):355-360.

28. Cramer EM, Meyer D, le Menn R, Breton-Gorius J. Eccentric localization of von Willebrand factor in an internal structure of platelet alpha-granule resembling that of Weibel-Palade bodies. *Blood*. 1985;66(3):710-713.

29. Sporn LA, Chavin SI, Marder V-J, Wagner DD. Biosynthesis of von Willebrand protein by human megakaryocytes. *J Clin Invest*. 1985;76(3): 1102-1106.

30. Ruggeri ZM, Dent JA, Saldívar E. Contribution of distinct adhesive interactions to platelet aggregation in flowing blood. *Blood*. 1999;94(1): 172-178.

31. Savage B, Almus-Jacobs F, Ruggeri ZM. Specific synergy of multiple substrate-receptor interactions in platelet thrombus formation under flow. *Cell*. 1998;94(5):657-666.

32. Stel HV, Sakariassen KS, de Groot PG, van Mourik JA, Sixma JJ. Von Willebrand factor in the vessel wall mediates platelet adherence. *Blood*. 1985;65(1):85-90.

33. Nichols TC, Samama CM, Bellinger DA, et al. Function of von Willebrand factor after crossed bone marrow transplantation between normal and von Willebrand disease pigs: effect on arterial thrombosis in chimeras. *Proc Natl Acad Sci USA*. 1995;92(7):2455-2459.

34. Verhenne S, Denorme F, Libbrecht S, et al. Platelet-derived VWF is not essential for normal thrombosis and hemostasis but fosters ischemic stroke injury in mice. *Blood*. 2015;126(14): 1715-1722.

35. Dent JA, Galbusera M, Ruggeri ZM. Heterogeneity of plasma von Willebrand factor multimers resulting from proteolysis of the constituent subunit. *J Clin Invest*. 1991;88(3): 774-782.

36. Furlan M, Robles R, Lämmle B. Partial purification and characterization of a protease from human plasma cleaving von Willebrand factor to fragments produced by in vivo proteolysis. *Blood*. 1996;87(10):4223-4234.

37. Savage B, Sixma JJ, Ruggeri ZM. Functional self-association of von Willebrand factor during platelet adhesion under flow. *Proc Natl Acad Sci USA*. 2002;99(1):425-430.

38. Yuan H, Deng N, Zhang S, et al. The unfolded von Willebrand factor response in bloodstream: the self-association perspective. *J Hematol Oncol*. 2012;5:65.

39. Ruggeri ZM, Orje JN, Habermann R, Federici AB, Reininger AJ. Activation-independent platelet adhesion and aggregation under elevated shear stress. *Blood*. 2006;108(6):1903-1910.

40. Savage B, Saldívar E, Ruggeri ZM. Initiation of platelet adhesion by arrest onto fibrinogen or translocation on von Willebrand factor. *Cell*. 1996; 84(2):289-297.

41. Ruggeri ZM, De Marco L, Gatti L, Bader R, Montgomery RR. Platelets have more than one binding site for von Willebrand factor. *J Clin Invest*. 1983;72(1):1-12.

42. Bryckaert M, Rosa J-P, Denis CV, Lenting PJ. Of von Willebrand factor and platelets. *Cell Mol Life Sci*. 2015;72(2):307-326.

43. Berliner S, Niiya K, Roberts JR, Houghten RA, Ruggeri ZM. Generation and characterization of peptide-specific antibodies that inhibit von Willebrand factor binding to glycoprotein IIb-IIIa without interacting with other adhesive molecules. Selectivity is conferred by Pro1743 and other amino acid residues adjacent to the sequence Arg1744-Gly1745-Asp1746. *J Biol Chem*. 1988; 263(16):7500-7505.

44. Weiss HJ, Hoffmann T, Yoshioka A, Ruggeri ZM. Evidence that the arg1744 gly1745 asp1746 sequence in the GPIIb-IIIa-binding domain of von Willebrand factor is involved in platelet adhesion and thrombus formation on subendothelium. *J Lab Clin Med*. 1993;122(3):324-332.

45. Massberg S, Gawaz M, Grüner S, et al. A crucial role of glycoprotein VI for platelet recruitment to the injured arterial wall in vivo. *J Exp Med*. 2003; 197(1):41-49.

46. Hewett PW, Murray JC. Human lung microvessel endothelial cells: isolation, culture, and characterization. *Microvasc Res*. 1993;46(1): 89-102.

47. Wong CHY, Jenne CN, Petri B, Chrobok NL, Kubes P. Nucleation of platelets with blood-borne pathogens on Kupffer cells precedes other innate immunity and contributes to bacterial clearance. *Nat Immunol*. 2013;14(8):785-792.

48. Beaulieu LM, Lin E, Morin KM, Tanriverdi K, Freedman JE. Regulatory effects of TLR2 on

megakaryocytic cell function. *Blood*. 2011; 117(22):5963-5974.

49. Pruss CM, Golder M, Bryant A, et al. Pathologic mechanisms of type 1 VWD mutations R1205H and Y1584C through in vitro and in vivo mouse models. *Blood*. 2011;117(16):4358-4366.

50. Savage B, Shattil SJ, Ruggeri ZM. Modulation of platelet function through adhesion receptors. A dual role for glycoprotein IIb-IIIa (integrin α IIb β 3) mediated by fibrinogen and glycoprotein Ib-von Willebrand factor. *J Biol Chem*. 1992;267(16): 11300-11306.

51. Goto S, Ikeda Y, Saldívar E, Ruggeri ZM. Distinct mechanisms of platelet aggregation as a consequence of different shearing flow conditions. *J Clin Invest*. 1998;101(2):479-486.

52. Wagner DD, Mayadas T, Urban-Pickering M, Lewis BH, Marder VJ. Inhibition of disulfide bonding of von Willebrand protein by monensin results in small, functionally defective multimers. *J Cell Biol*. 1985;101(1):112-120.

53. Zhou W, Inada M, Lee TP, et al. ADAMTS13 is expressed in hepatic stellate cells. *Lab Invest*. 2005;85(6):780-788.

54. Schaff M, Tang C, Maurer E, et al. Integrin $\alpha_6\beta_1$ is the main receptor for vascular laminins and plays a role in platelet adhesion, activation, and arterial thrombosis. *Circulation*. 2013;128(5): 541-552.

55. van Schooten CJ, Shahbazi S, Groot E, et al. Macrophages contribute to the cellular uptake of von Willebrand factor and factor VIII in vivo. *Blood*. 2008;112(5):1704-1712.

56. Ware J, Russell SR, Marchese P, Ruggeri ZM. Expression of human platelet glycoprotein Ib alpha in transgenic mice. *J Biol Chem*. 1993; 268(11):8376-8382.

57. Spor A, Koren O, Ley R. Unravelling the effects of the environment and host genotype on the gut microbiome. *Nat Rev Microbiol*. 2011;9(4): 279-290.

58. Koeth RA, Wang Z, Levison BS, et al. Intestinal microbiota metabolism of L-carnitine, a nutrient in red meat, promotes atherosclerosis. *Nat Med*. 2013;19(5):576-585.

59. Wieberdink RG, van Schie MC, Koudstaal PJ, et al. High von Willebrand factor levels increase the risk of stroke: the Rotterdam study. *Stroke*. 2010;41(10):2151-2156.

60. Seaman CD, Yabes J, Comer DM, Ragni MV. Does deficiency of von Willebrand factor protect against cardiovascular disease? Analysis of a national discharge register. *J Thromb Haemost*. 2015;13(11):1999-2003.

61. Zhu W, Gregory JC, Org E, et al. Gut microbial metabolite TMAO enhances platelet hyperreactivity and thrombosis risk. *Cell*. 2016;165(1):111-124.

62. Yano JM, Yu K, Donaldson GP, et al. Indigenous bacteria from the gut microbiota regulate host serotonin biosynthesis [published correction appears in Cell. 2015;163(1):258]. *Cell*. 2015; 161(2):264-276.

63. Spadoni I, Zagato E, Bertocchi A, et al. A gut-vascular barrier controls the systemic dissemination of bacteria. *Science*. 2015; 350(6262):830-834.

64. Pan J, Dinh TT, Rajaraman A, et al. Patterns of expression of factor VIII and von Willebrand factor by endothelial cell subsets in vivo. *Blood*. 2016; 128(1):104-109.